A PIN Diode Model for Finite Element Time Domain Simulations

Diogenes Marcondes F., Wilson A. Artuzi Jr., Marlio J. C. Bonfim

Departamento de Engenharia Elétrica - Universidade Federal do Paraná

Abstract— **This work presents an equivalent circuit model for a PIN diode to be used with finite element electromagnetic simulations in time domain. The proposed model includes low and high frequency behaviors. The parameters of a commercial PIN diode are extracted from measurements and a single pole single through switch is constructed. The obtained results show the consistence and applicability of the proposed model.**

Keywords— **PIN diode, finite element method, RF switch**

I. Introduction

The finite element time domain (FETD) method has been recognized as a powerful tool to predict the behavior of electromagnetic wave in radio frequency (RF) and microwave structures of complex geometry [1]. Its extension to deal with lumped elements allows the analysis of more sophisticated devices having electronic components embedded. Models of transistors and diodes have been successfully implemented in extended FETD codes [2], but the extension to include a model for the PIN diode, which is the basic component of voltage controlled attenuators and switches, has not been reported thus far.

The PIN diode is a unique device that can handle high power electromagnetic waves using low current intensity for control [3]. This is accomplished by the presence of an intrinsic semiconductor region placed between P and N doped regions. At high frequencies, the intrinsic region provides a linear junction conductance and reduces the junction capacitance, therefore the PIN diode is suitable for the implementation of attenuators and switches at RF and microwave frequencies. The main drawback in finding a consistent model for the PIN diode is its complicated transition from low to high frequency states, therefore its model is not available in popular circuit simulators. In practice, however, this region of transition is useless and the model can be separated in two parts: one for low frequencies and other for high frequencies.

The objective of this paper is to present two equivalent circuit models of a PIN diode, one at low and other at high frequencies and couple only the high frequency model to the unconditionally stable FETD framework [4]. Measurements employing a commercial PIN diode have been conducted to extract both low and high frequency circuit parameters. Results of simulations in comparison with measurements show the consistence of the proposed model.

This work is partially supported by Fundação Araucária with a PIBIC research grant to Diogenes Marcondes F. Contacts: diogenesmf@yahoo.com.br, artuzi@eletrica.ufpr.br, marliob@eletrica.ufpr.br.

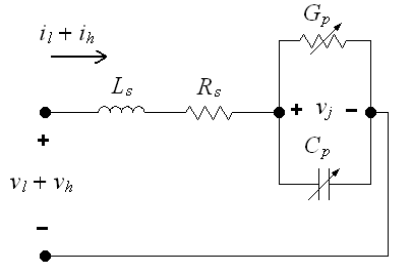

Fig. 1. Equivalent circuit model of a PIN diode.

II. Equivalent Circuit Models

A. Low Frequency Model

At low frequencies, the PIN diode behaves as a conventional PN junction diode [3]. The complete equivalent circuit, including lead resistances and inductances is shown in Fig. 1, whose behavior is governed by

$$v_l = (sL_s + R_s)\, i_l + v_j \tag{1}$$

where $s = j2\pi f$ is the complex frequency, v_l is the external low frequency voltage source, v_j and i_l are the junction voltage and current, respectively at low frequencies, R_s and L_s are leads resistance and inductance, respectively. The current i_l has a nonlinear characteristic depending on the junction voltage as

$$i_l = (1 + s\tau)\, i\,(v_j) + s\; q\,(v_j) \quad . \tag{2}$$

The nonlinear dependences of the current $i\,(v_j)$ in G_p and the depletion charge $q\,(v_j)$ in C_p are given by

$$i\,(v_j) = I_S \left(e^{\frac{v_j}{V_T}} - 1 \right) . \left(e^{\frac{v_j - V_N}{2V_T}} + 1 \right)^{-1} \tag{3}$$

$$q\,(v_j) = C_{J0} \left[v_j + |v_j| - \left(\frac{V_J}{1-M} \right) . \left(1 + \frac{|v_j|}{V_J} \right)^{1-M} \right] \tag{4}$$

where I_S, V_T, V_J, C_{J0} and M are parameters that have their corresponding meanings in conventional PN junction diodes. The diffusion charge is appears in (2) given by the parameter τ (average minority carrier lifetime). The last product term in (3) has been introduced in order to represent correctly the carrier injection coefficient variation from 1 to 2 being V_N the transition voltage.

B. High Frequency Model

As frequency increases, the period of the current through the junction approaches the carrier recombination time and the net charge in the intrinsic region of the PIN diode vanishes. Consequently, the unbiased PIN diode behaves as a capacitor at high frequencies. If a low frequency current bias is enforced through the intrinsic region, carriers are injected and the PIN diode acts as a linear resistor at high frequencies, but controlled by the intensity of the low frequency current bias. Thus, at high frequencies, the PIN diode can be represented by the same equivalent circuit of Fig. 1, but with linear C_p and G_p elements determined by the low frequency junction voltage v_j, as

$$G_p(v_j) = \frac{8}{3}\left(\frac{L}{W}\right)^2 \frac{di(v_j)}{dv_j} \quad (5)$$

$$C_p(v_j)^{-1} = \frac{W}{\varepsilon A} + \left[\frac{dq(v_j)}{dv_j}\right]^{-1} \quad (6)$$

where W and A are the intrinsic region length and cross-sectional area, respectively, L is the ambipolar diffusion length and ε electric permittivity [3]. Since the ratios W/L and $W/\varepsilon A$ are not known, they must be evaluated experimentally. The high frequency model is governed by

$$v_h = \left[sL_s + R_s + \frac{1}{sC_p(v_j) + G_p(v_j)}\right] i_h \quad . \quad (7)$$

III. Finite Element Method

The finite element procedure applied to the electric field vector wave equation using edge linear basis functions [5] results in an equivalent electric circuit matrix equation of the form

$$\left(sC + G + \frac{1}{s}K\right) v + p\ i_h = i_s \quad (8)$$

where the entries of vectors i_s and v are the known excitation current sources and the unknown voltages on the edges of the finite element mesh, respectively [4]. The entries of matrices C, G and K relate pairs of basis functions $\vec{W}_k$ and $\vec{W}_l$ as

$$C_{kl} = \int_V \varepsilon \vec{W}_k . \vec{W}_l \ dV \quad (9)$$

$$G_{kl} = \oint_S \sigma_s \ \hat{n} \times \vec{W}_k . \hat{n} \times \vec{W}_l \ dS \quad (10)$$

$$K_{kl} = \int_V \frac{1}{\mu} \nabla \times \vec{W}_k . \nabla \times \vec{W}_l \ dV \quad (11)$$

where ε and μ are the electric permittivity and magnetic permeability in the computational domain V and σ_s is the surface conductivity of the domain boundary S being $\hat{n}$ the normal unit vector outward S. The PIN diode is assumed to be connected in parallel with one edge of the mesh, thus the entries of vector p are all zeros except for the value one in the row corresponding to the edge where the diode is placed and the high frequency voltage applied to the diode is the voltage across its corresponding edge given by

$$v_h = p^T v \quad (12)$$

where T denotes the transposed vector.

In order to solve (8) in the discrete time domain, it will be convenient to make

$$v = s\ w \quad (13)$$

and add the term

$$\frac{1}{L_s} p\ p^T w \quad (14)$$

to both sides of (8) to form, together with (7), the system of equations

$$\left[s^2 C + sG\ + K + \frac{1}{L_s} p\ p^T\right] w\ = i_s - p\ i_h + \frac{1}{L_s} p\ p^T w \quad (15)$$

$$\left[s^2 L_s + sR_s + \frac{s}{sC_p(v_j) + G_p(v_j)}\right] i_h = p^T w \quad (16)$$

To solve (15) and (16) in the discrete time domain, the bilinear transformation

$$s = \frac{2}{\Delta t} \frac{1 - z^{-1}}{1 + z^{-1}} \quad (17)$$

is applied and the inverse z transform given by the property

$$z^{-k} . w(z) \leftrightarrow w^{n-k+1} \quad (18)$$

maps to the discrete time instant $t = (n - k + 1)\Delta t$ being Δt the time step [6]. After some algebraic manipulations, the system of equations (15) and (16) can be written as the set of recurrence relations

$$Q\ u^n = i_s^n - p\ i_h^n - G\ v^{n-1/2} - K\ w^n \quad (19)$$

$$v^{n+1/2} = v^{n-1/2} + \Delta t\ u^n \quad (20)$$

$$w^{n+1} = w^n + \Delta t\ v^{n+1/2} \quad (21)$$

$$i_h^{n+1} = \frac{b_1}{a_2} p^T v^{n+1/2} + \frac{b_0}{a_2} p^T v^{n-1/2} - \frac{a_1}{a_2} i_h^n - \frac{a_0}{a_2} i_h^{n-1} \quad (22)$$

with

$$Q = C + \frac{\Delta t}{2} G + \frac{\Delta t^2}{4}\left(K + \frac{1}{L_s} p p^T\right) \quad (23)$$

$$a_2 = \frac{L_s C_p}{\Delta t^2} - \frac{L_s G_p + R_s C_p}{2\Delta t} + \frac{R_s G_p + 1}{4} \quad (24)$$

$$a_1 = -\frac{2L_s C_p}{\Delta t^2} + \frac{R_s G_p + 1}{2} \quad (25)$$

$$a_0 = \frac{L_s C_p}{\Delta t^2} + \frac{L_s G_p + R_s C_p}{2\Delta t} + \frac{R_s G_p + 1}{4} \quad (26)$$

$$b_1 = \frac{G_p}{2} + \frac{C_p}{\Delta t} \quad (27)$$

$$b_0 = \frac{G_p}{2} - \frac{C_p}{\Delta t} \quad . \quad (28)$$

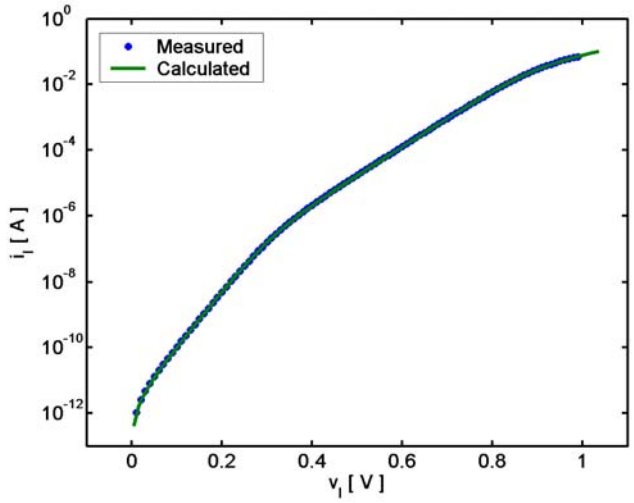

Fig. 2. IxV curve of the 1SV172 PIN diode: • measured, — fitted.

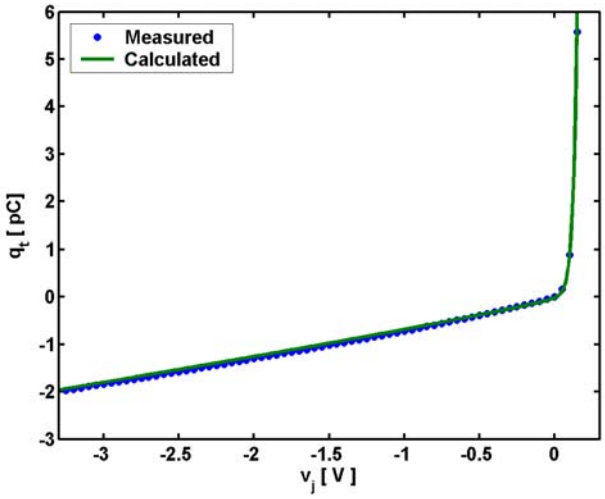

Fig. 3. QxV curve of the 1SV172 PIN diode: • measured, — fitted.

The system of linear equations (23) is solved employing the conjugate gradient method with diagonal preconditioning and using seven iterations per time step [4]. The unknown voltage vector is updated in (20) and the high frequency current in the PIN diode is updated in (22).

IV. Results

In order to verify the consistence of the proposed models for the PIN diode, the commercial 1SV172 PIN diode pair has been investigated. First, the low frequency parameters are extracted from measurements with the Agilent 4155C Semiconductor Parameter Analyzer. Next, a single pole single through switch is constructed and measured at 500 MHz to obtain the remaining high frequency parameters.

A. Low Frequency Parameters

To perform the low frequency measurements, thin wire leads are soldered to the terminals of one of the two diodes in the package and connected to a calibrated text fixture. The semiconductor parameter analyzer is able to measure the IxV and the QxV curves as shown in Figs. 2 and 3, respectively.

From the measured IxV curve, the parameters I_S, V_N and R_s can extracted using the procedure below, assuming $V_T = 25\text{mV}$.

1. Use (3) with $V_N = 100$ V to adjust I_S in the range $v_j = v_l < 0.1$ V.
2. Use (3) with I_S obtained above to adjust V_N in the range $v_j = v_l < 0.7$ V.
3. Use (1) with $L_s = 0$, and with I_S and V_N obtained above to adjust R_s in the range $v_l < 1.0$ V.

The obtained values of $I_S = 2.1$ pA, $V_N = 0.3$ V and $R_s = 1\ \Omega$ have been used to plot the calculated curve in the graph of Fig. 2. It is clear in the figure the change of the curve slope at $v_l = V_N = 0.3$ V due to the change of the carrier injection coefficient from 1 to 2.

From the measured QxV curve, the parameters V_J, C_{J0}, M and τ are extracted. In this case, it is convenient to use the total charge equation

$$q_t(v_j) = q(v_j) + \tau\ i(v_j) + q_0 \tag{29}$$

where the term $q_0 = -q(0) - \tau i(0)$ is added to provide $q_t(0) = 0$, in accordance with the measured curve. In this case, the parameters have been found by trial and error due to the complexity of the equation. Nevertheless, any nonlinear optimization algorithm could be used instead.

The obtained values of $V_J = 25$ mV, $C_{J0} = 0.86$ pF, $M = 0.1$ and $\tau = 7$ ms have been used to plot the calculated curve in the graph of Fig. 3. The parameter τ establishes the curve slope in the forward bias region while the parameter V_J is responsible for the smoothness of the transition from reverse to forward bias.

B. High Frequency Parameters

The high frequency parameters are obtained from the measurement of the transmission coefficient of a single pole single through switch as a function of the DC voltage applied to the PIN diode.

The schematic circuit of the switch is shown in Fig. 4. A DC voltage source with 75 Ω internal resistance is used as the low frequency voltage source. For convenience of construction, both diodes of the package are biased, but only one acts as the RF switch. The RF sinusoidal source with 5 0Ω internal resistance is provided by the Agilent E4432B Signal Generator at 500 MHz which is represented by the current source in parallel with a 50 Ω resistor, as shown in Fig. 4. The output voltage is monitored by a the LeCroy LT584 Digital Storage Oscilloscope with 50 Ω internal resistance which is represented by a 50 Ω resistive load in Fig. 4. An inductor and two capacitors provide the necessary DC and RF decoupling.

The switch is mounted on a FR4 substrate having 1.27 mm of thickness and a dielectric constant of 4.5, as depicted

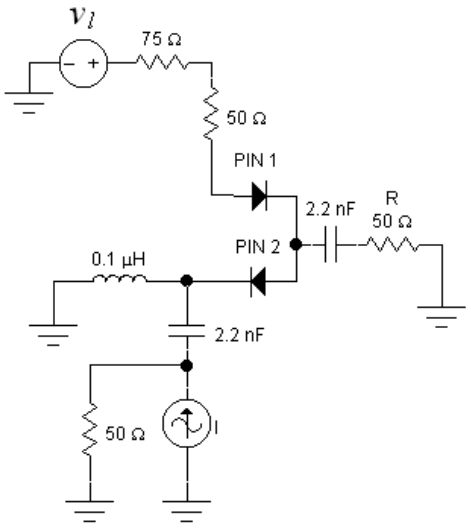

Fig. 4. Schematic circuit of the single pole single through switch using the 1SV172 diode pair.

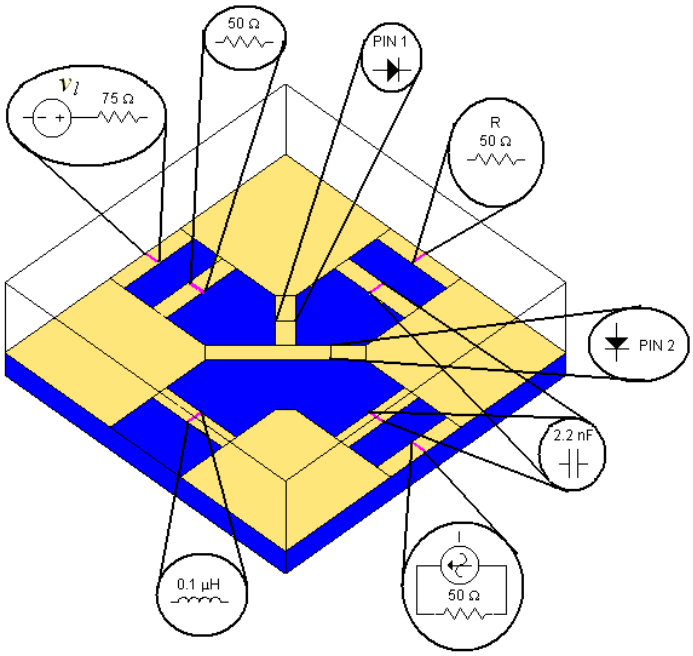

Fig. 5. Structure of the single pole single through switch using the 1SV172 diode pair.

in Fig. 5. The bottom side is metallized and on the upper side a cross formed by two metallic strips having 2.5 mm of width are etched with 0.5 mm gaps conveniently placed to solder the lumped elements. Three BNC connectors are soldered at the ends of the strips to connect the outputs of the external sources and the input of the oscilloscope.

The magnitude of the transmission coefficient is obtained as the ratio of the RMS voltages read in the oscilloscope with the switch connected and with a through bypass connected in the place of the switch. The measured results are shown in Fig. 6. An insertion loss of 2 dB and an isolation of 18 dB have been obtained when the switch is ON and OFF, respectively. The insertion loss is bounded by losses in R_s and by the high frequency leakage through the biasing circuitry. The isolation bounded by high frequency leakage through C_p. The optimization of the switch performance has not been addressed in this work, though it can be done in future.

Simulations have been performed using a time step of 1.4 ps and a finite element mesh with tetrahedral elements having an average edge length of 1.5 mm. To include lumped capacitors, resistors and inductors, their capacitances, conductances and the inverse of inductances are added to the main diagonal of matrices C, G and K, respectively, in the positions corresponding to edges of mesh where they are placed. Metallic surfaces have been modelled with $\sigma_s = 10^6$ S. An air layer with a thickness of 2.5 mm bounded by perfect magnetic walls ($\sigma_s = 0$) is included. Absorbing boundary conditions are not necessary in this case because the structure is small compared to a wavelength, thus unwanted radiation can be neglected.

The high frequency parameters W/L and $W/\varepsilon A$ have been chosen to match simulated and measured curves, as shown in the graph of Fig. 6. First, the parameter $W/L = 0.81$ has been found using $W/\varepsilon A = 0$ and $v_l = 1.1$ V. In this

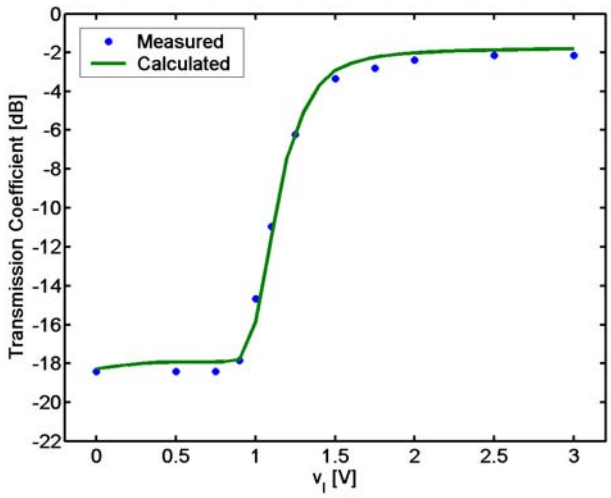

Fig. 6. Single pole single through switch transmission coefficient against DC control voltage: • measured, — calculated.

range of v_l, G_p has a predominant effect over C_p and R_s. Next, the parameter $W/\varepsilon A = (0.46\text{ pF})^{-1}$ has been found using $W/L = 0.81$ and $v_l = 0$. In all simulations, for each given value of v_l, the corresponding value of v_j, necessary in (7), has been found numerically using the Newton's method to solve (1) with $s = 0$ because a DC bias is applied. As it can be observed in Fig. 6, the simulated curve agrees with the measured results for the other values of v_l different than those used to estimate the high frequency parameters.

V. Conclusions

A PIN diode has been modelled by two equivalent circuits, one for low and other for high frequencies. The high frequency model is coupled with the FETD framework using the bilinear transformation to obtain the discrete time recursive equations. The low frequency model has accurately represented the behavior of a commercial PIN diode and the construction of a single pole single through PIN diode switch provided the extraction of the two unknown parameters of the high frequency model with the aid of FETD simulations. Using the extracted PIN diode parameters, the simulated transmission coefficient of the switch matched the measured results as a function of the control voltage at 500MHz.

The frequency dependence of the transmission coefficient and the transient behavior of the switch are important aspects that need to be evaluated in future to conclude this work.

References

[1] J-F. Lee, "WETD-A finite element time-domain approach for solving Maxwell's equations", *IEEE Microwave and Guided Wave Letters*, vol. 4, pp. 11-13, Jan. 1994.

[2] H-P. Tsai, Y. Wang and T. Itoh, "An unconditionally stable extended (USE) finite-element time-domain solution of active nonlinear microwave circuits using perfectly matched layers", *IEEE Trans. on Microwave Theory and Techniques*, vol. 50, pp. 2226-2232, Oct. 2002.

[3] I. Bahl and P. Bhartia, *Microwave Solid State Circuit Design*, John Wiley & Sons, 1988.

[4] W. A. Artuzi Jr., "Improving the Newmark time integration scheme in finite element time domain methods," *IEEE Microwave and Wireless Comp. Lett*, vol.15, pp.898-900, Dec. 2005.

[5] J. P. Webb, "Edge elements and what they can do for you," *IEEE Trans. Magn.*, vol.29, pp.1460-1465, Mar. 1993.

[6] A. V. Oppenheim, R. W. Schafer and J. R. Buck, *Discrete-Time Signal Processing*, Prentice-Hall, 1999.